Journal of Umm Al-Qura University for Applied Science

journal homepage: https://uqu.edu.sa/en/jas/87823

Nanocomposite containing polyamide and GNS for enhanced properties. Synthesis and characterization

Gadeer Ashour [a,b*], Mahmoud Hussein[a,c] and, Tariq Sobahi [a]

[a] *Chemistry Department, Faculty of Science, King Abdulaziz University, Jeddah, Saudi Arabia.*
[b] *Chemistry Department, Faculty of Applied Science, Umm Al-Qura University, Makkah, Saudi Arabia.*
[c] *Chemistry Department, Faculty of Science, Assiut University, Assiut, Egypt.*

ARTICLE INFO

Article History:
Submission date: 12-9-2021
Accepted date: 13-10-2021

Keywords:
Polyamide derivatives, Polymer synthesis, Nanocomposite, thermal properties, GNSs.

ABSTRACT

A new series of nanocomposite containing polyamide and graphene nanosheets PAS/GNSs$_{a-d}$ has been fabricated based on different weight proportions of GNS (1%, 3%, 5% and 10%) throughout the same experimental procedure. Before that the polymerization procedure was successfully produce polyamide which include sebacoyl derivative (PAS) through low-temperature polycondensation method. The polymerization was occurred by the interaction between the previously synthesized monomer 2, aminothiazole diphenylsulfide M2 and sebacoyl chloride in dimethylformamide DMF with potassium carbonate anhydrous K_2CO_3 as a catalyst. Additionally, the desired PAS/GNSs$_{a-d}$ nanocomposites were characterized through certain characterization tools, including FT.IR, solubility, gel permeation chromatography GPC, and X-ray diffraction analysis XRD. Thermogravimetric data displayed a strong enhancement in the thermal stability behavior of PAS/GNSs$_{a-d}$ with the different GNS percentages. Moreover, the morphology measurements for chosen nanocomposites polymers were evaluated by using scanning electron microscope SEM and transmission electron microscope TEM, which detected the formation of PAS/GNSs$_{b,d}$. The images from the TEM demonstrated a homogeneous distribution of the GNS throughout the polymer matrix.

1. Introduction

Polymer nanocomposites are made up of two different components, the first of which is concerned with the organic matrix (in this case, polymers), and the second is concerned with the nanomaterials (nanofiller) that are combined on a macroscopic scale [1]. These classes have been quite important in recent years because of the qualities that the final material affects. The final materials combine the characteristics of each component leads to cover a wide range of industrial applications, especially low density, low cost, high efficient biological activity along with massive environmental sustainability, interesting sensing eventuality, electrostatic discharge, mechanical performance, incredible coating performance, high operating temperature range and photoconductivity for electronics and other amazing properties mentioned in the literature [2-8]. Nanofillers with a few percent or less amount of carbon black, carbon nanomaterials, silica, metal and metal oxide or others are used to increase the polymers' physical, chemical, thermal, optical, and mechanical characteristic features [9-11]. Additionally, good distribution and significant transmission intensity through interfacial areas are required for optimal performance [12,13]. Moreover, graphene and carbon nanotubes CNTs are examples of carbon nanomaterials which have wide attention in various fields owing to their remarkable properties such as low density (1.2-2g/cm^3) with Young's modulus (~130 GPa and ~1 TPa, respectively) and ultrahigh strength [10,14,15]. It is important to know that the graphene nanosheets (GNSs) have electrical behaviors, making them appropriate to change the conducting behavior of any material. Moreover, CNTs and GNSs were used in several industrial fields such as catalysts, solar cells, sensors, inorganic pollutant treatment, medical applications, fuel cells, photonics, and composites [14].

Polyamides (PAs) are engineering thermoplastics that have a lot of outstanding features instance high strength, good barrier properties, abrasion resistance, and elasticity. The essential applications areas of polyamides are in films and coatings, electrical equipment, automotive parts, and electronic products. However, polyamides still have a number of drawbacks due to consist a numerous amide hydrogens and carbonyl oxygens which can form readily hydrogen bonds [16]. Therefore, the presence of thiazole ring in the sulfur-based polymers has an important role [17]. First of all, the thiazole is a heterocyclic ring containing nitrogen and sulfur atoms. Thiazole derivatives are widely used as bioactive agents, liquid crystals, sensors, catalysts, etc [18]. In addition, introduce the thiazole ring as the nucleus of the derivatives considered from a medicinal chemistry perspective [19]. Thiazole-containing polyamides exhibit fire retarding properties, electronic conductivity, chemical resistance, high thermal stability, high mechanical properties, photo-curing properties, and biological activity [20,21]. Recently, much more attention has been given to nanofillers on sulfur-containing polymer chains. A new category of polyazomethine/graphene nanocomposites and polyazomethine/multi-wall carbon nanotubes was synthesized, which exhibited the conducting properties [22,23].

In this research, the major aim is to study nanofillers' effect on polyamide chains and evaluate (GNSs). Synthesis of polyamide and its nanocomposites PAS/GNSs$_{a-d}$ is a requirement to achieve this aim. Both structures of pure polyamide (PAS) and related nanocomposites PAS/GNSs$_{a-d}$ were confirmed by FT-IR measurements. Then, all new polymers were investigated through typical characterization tools such as thermal analysis, X-ray diffraction analysis, scanning electron microscope and transmission electron microscope. This is as we mentioned earlier because the thiazole containing polyamides have various interesting features, besides, the electrical behavior of (GNSs) makes them a good material of conducting polymers.

2. Results and discussion

2.1. Chemistry and characterization tools

The target polyamide derivative PAS was fabricated with various percentages of GNSs using in-situ polycondensation polymerization process. Before polymerization the monomer M1 bis-4-chloroacetyl-diphenylsulfide and monomer M2 2-aminothiazole-diphenylsulfide were prepared as presented in the experimental section. The obtained monomers have been measured the melting point by An Automated

* **Corresponding Author**
Chemistry Department, Faculty of Applied Science, Umm Al-Qura University, Makkah, Saudi Arabia.
E-mail address: **grashour@uqu.edu.sa** (Gadeer Ashour).

Melting Point Apparatus with a Digital Image Processing Technology, and the result was in agreement with the results obtained in [24,25]. Besides, their chemical structures were characterized using spectral common techniques such as NMR and FT.IR, that showed the expected structures as presented in the experimental section. The synthetic route for synthesizing the PAS/GNSs$_{a-d}$ nanocomposites by in-situ polymerization procedure is demonstrated in Figure 1.

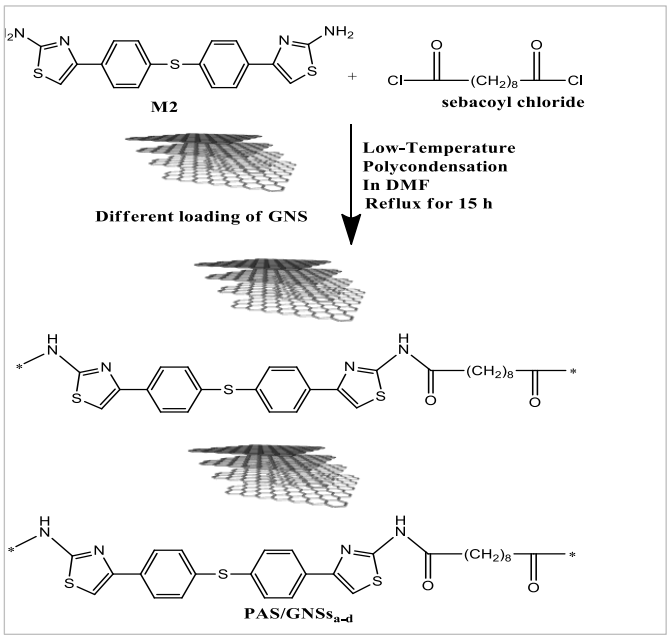

Figure 1. synthesis process of the polyamide nanocomposites PAS/GNSs$_{a-d}$.

The polymerization reactions are the same way as the polymerization procedure for pure polyamide. The fabrication process is based chiefly on fixed weight 2-aminothiazole diphenylsulfide M2 and sebacoyl chloride in the presence of various loading of GNSs. The chemical structure of these new nanocomposites was gained using also FT.IR spectroscopy. As a result, the polymers showed absorption bands at 3113-3122 cm^{-1} (NH of urea derivative) and 1615 cm^{-1} (C=O of urea derivative). The FT.IR measurements show apparent proof for the physical interaction between PAS and the GNSs (a, b, c, d) nanomaterials, which is considered as a recognized way of bonding between the polymer matrix and its nanofiller. Figure 2 (a) spectrum gives intensive characteristic absorption bands for pure PAS, and (b-e) gives the FT.IR spectrums for PAS/GNSs$_{a-d}$ nanocomposites. The spectrum of PAS/GNSs$_{a-d}$ nanocomposites is clearly observed that the absorption bands as same as the spectra of pure PAS, but there are somewhat changes in the spectrum of pure polyamide after immersion of the GNSs into PAS polymer matrix. The absorption bands of GNSs are prominent in the spectra of our nanocomposites [23].

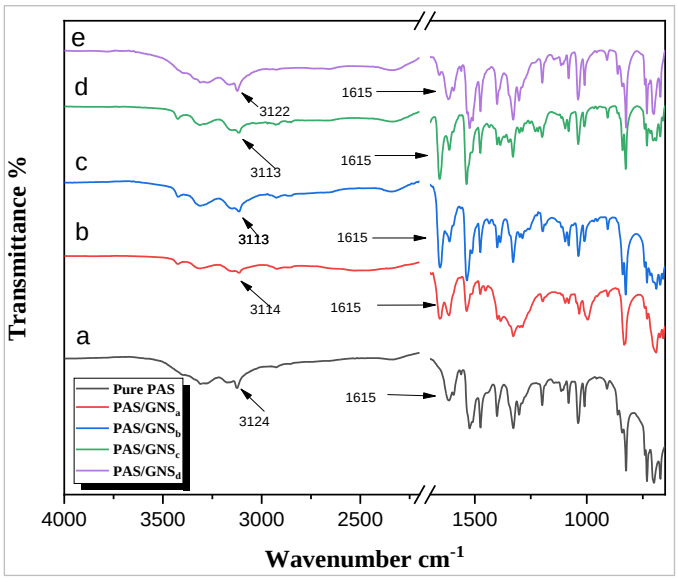

Figure 2. FT.IR of pure PAS and PAS/GNS$_{a-d}$.

2.2. Enhance properties

The following general methods characterized the new polyamide and its fabricated nanocomposites: solubility and gel permeation chromatography GPC. The solubility of polyamide was evaluated at ambient temperature using many organic solvents such as protonic solvents, aprotic solvents, and non-polar solvents. The polyamide PAS was strongly soluble in concentrated HCOOH and in concentrated H_2SO_4 as a protonic solvent. In addition, PAS was soluble in THF, DMF, DMSO, and acetone as organic aprotic solvents, whereas they were partially soluble in other aprotic organic solvents such as DCM and chloroform. The polyamide showed bad solubility behavior in benzene as non-polar solvents. Table 1 offerings the solubility behavior for the produced polyamide PAS in various solvents. This observation is owing to the presence of hetero aromatic sulfur ring (thiazole ring) units in the main chain of the polyamides [21].

Table 1. Solubility characteristics of PAS.

Polymer code	THF	DMF	Formic acid	$CHCl_3$	DCM	DMSO	Sulfuric acid	Benzene	Acetone
PAS	+	+	+	+ −	+ −	+	+	−	+

+ Soluble at room temperature.
+ − Partially soluble.
− Insoluble.

The GPC gel permeation chromatography is a common technique used for measuring molecular weight. This molecular weight of PAS was measured by GPC, as clarified in the experimental section. The value was recorded and calculated by a computer program [7,23, 26, 27]. The average number, weight average molecular weights, and polydispersity index, and the average number of repeating units (Mw, Mn, Pw, and PDI) of polyamide were measured, and their data are represented in Table 2. According to the outcomes, it was found that the polyamide has a medium chain (Mw = 38591.55) [22].

Table 2. The GPC results for PAS.

sample	formula	GPC results			
		[a]Mw	[b]Mn	[c]Pw	PDI
PAS	$C_{28}H_{28}O_2S_3N_4$	38591.55	34458.24	~ 70	1.12

[a]Weight-average molecular weight
[b]Number-average molecular weight
[c]Average number of repeating units

XRD and TGA also characterized the produced polyamide and its related nanocomposites to determine the crystallinity and the thermal stability, respectively. The thermal properties of sulfur-containing polyamide PAS and its fabricated PAS/GNSs$_{a-d}$ were evaluated by TGA, as seen in Figure 3. Various temperatures for various percentage weight losses of pue PAS and PAS/GNSs$_{a-d}$ nanocomposites are presented in Table 3, in which values of T_{10}-T_{40} denote the temperatures for variable weight losses % at 10%, 20%, 30%, and 40%. The PAS and PAS/GNSs$_{a-d}$ nanocomposites were heated up to 800°C at the rate of 10°C/min in N_2 atmosphere and showed multi-step processes decomposition. The TG curves showed the loss of moisture tied solvents, which might lose a small weight in the range 1% and 5% for PAS/GNS$_{a-c}$, pure PAS and PAS/GNS$_d$, respectively. This step starts at ambient temperature and ends before 100°C for PAS/GNS$_{a-c}$ nanocomposites and ends at around 294°C for pure PAS and PAS/GNS$_d$. The decomposition for PAS/GNS$_{a-c}$ is led to the nature of these polymers and occurs mainly in overlapped one step in the range of 100-185°C. The first decomposition step starts at 100 and ends at 272°C. Additionally, the second decomposition step starts at 279 and ends at 424°C, and the third decomposition step starts at 446 and ends at 600°C.

The second step indicates the decomposition of polymers due to pyrolytic oxidation of (C=C) that separate from many bonds with the elimination of free shorter chains depending on the nature of these polymers and creation of char as end products [21, 27]. In general, the decomposition in the second step is faster than the decomposition in the first step. On the other side, the pure PAS and PAS/GNS$_d$ show considerable separation between the two degradation steps. The first decomposition step starts at 300°C and ends at 408°C. The second decomposition step starts at 440°C and ends at 560°C. The solid residue left (char end products) at around 670°C. In Table 3, various % weight losses percentage at 10, 20, 30, and 40 in $T_{10} - T_{40}$ temperature values.

Table 3. Thermal Properties of pure PAS and PAS/GNSs$_{a-d}$.

			Temperature (°C) for various percentage decompositions			
code	IDT[a]	FDT[a]	10%	20%	30%	40%
PAS	334.9	630.9	367	470	562	679
PAS/GNS$_a$	103.65	630.9	165	239	434	569
PAS/GNS$_b$	103.65	630.9	172	391	482	583
PAS/GNS$_c$	103.65	630.9	264	415	508	628
PAS/GNS$_d$	334.9	630.9	356	463	563	698

[a]The values were determined by TG curves at heating rate of 10°C/min

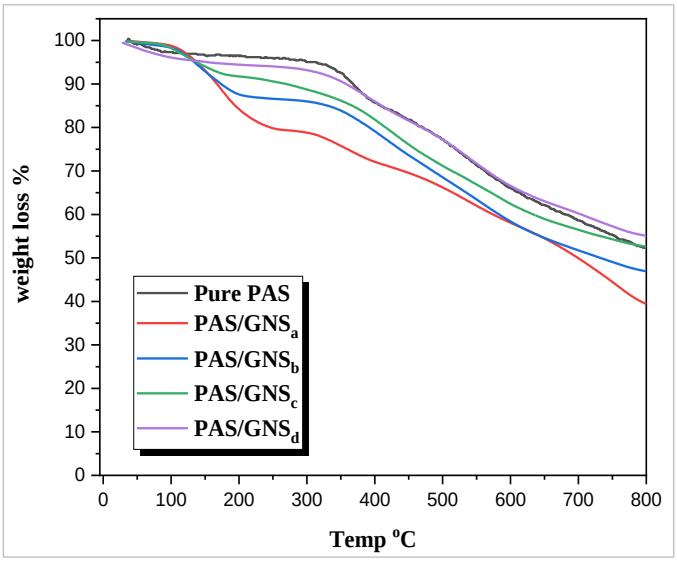

Figure 3. TGA curves of Pure PAS/GNSs$_{a-d}$ (1%, 3%, 5%, 10%) at a heating rate of 10°C/min.

X-ray Diffractograms were detected by X-ray Diffractometer model type (RIGAKU ULTIMA_IV) (Mannai Technical Services) over the 2θ region = 10-80°C. The data confirms the nature of pure PAS and its nanocomposites PAS/GNSs$_{a-d}$, as presented in Figure 4. The pattern of PAS was changed from semi crystalline to crystalline in the nanocomposite polymers with increased GNS ratio. Most likely, the bulky hetero-cyclic rings throughout the polyamide backbone are the fundamental reason of their crystallization properties. It is possible to determine the order of crystallinity based on the presence of a polar C=O as well to several C=C bonds. The orneriness and hence crystallinity are the results of this condition [28]. In addition, the formation of our selected composites products was clearly elucidated by XRD diffractograms for all PAS/GNS$_{a-d}$ nanocomposites with various GNS loading. The GNSs present a diffraction peak at around 22° attributed to amorphous carbon material and around 26° (002) related to graphite planes [29, 30].

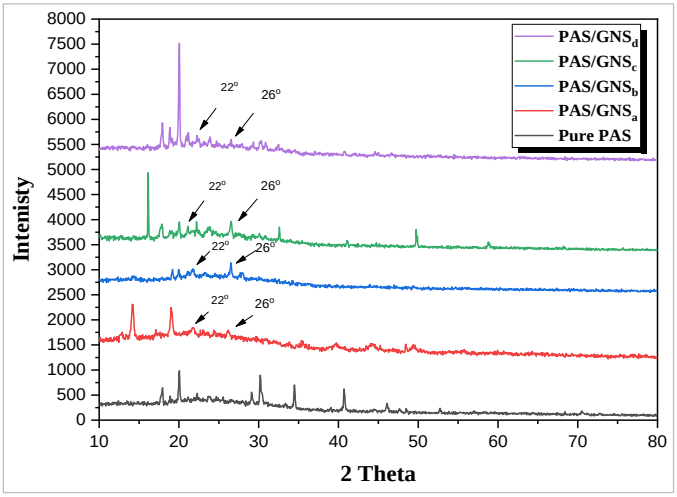

Figure 4. XRD of PAS/GNSs$_{a-d}$ (1%, 3%, 5%, 10%).

The morphologies of new polyamide and its nanocompos ites were studied by SEM and TEM measurements. The SEM images of chosen samples PAS/GNS$_b$ and PAS/GNS$_d$ were illustrated in Figure 5. At low magnification X= 800, the PAS/GNS$_b$ surface were flower shape, with aggregation of GNS on the polymer surface. In addition, at magnification of X= 1500-3000 in PAS/GNS$_d$ the morphology of the surface as same as flowers covered with thin slices of 10 wt.% GNSs. However, these structures were destroyed when magnification was increased. These morphological properties exposed excellent homogenous size distribution of GNS on the surface of polyamide.

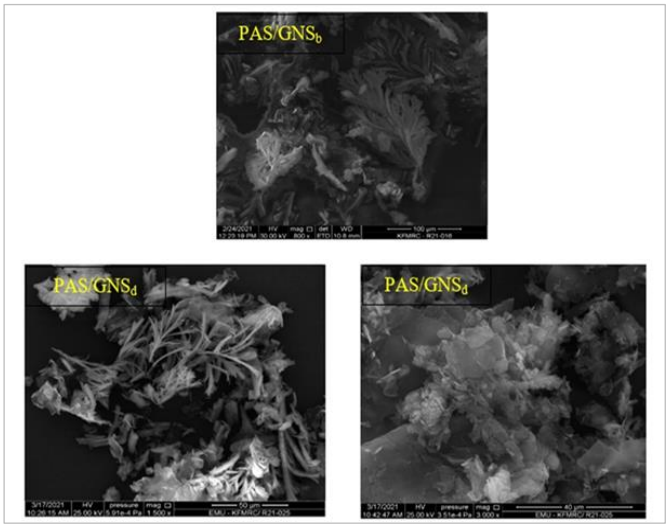

Figure 5. SEM images for PAS/GNS$_b$ and PAS/GNS$_d$.

The TEM morphologies of PAS/GNS$_{b,d}$ in Figure 6 exhibited that the GNS immersed with polyamide with homogenous size, shape, and distribution without aggregation or concentration in any specific areas.

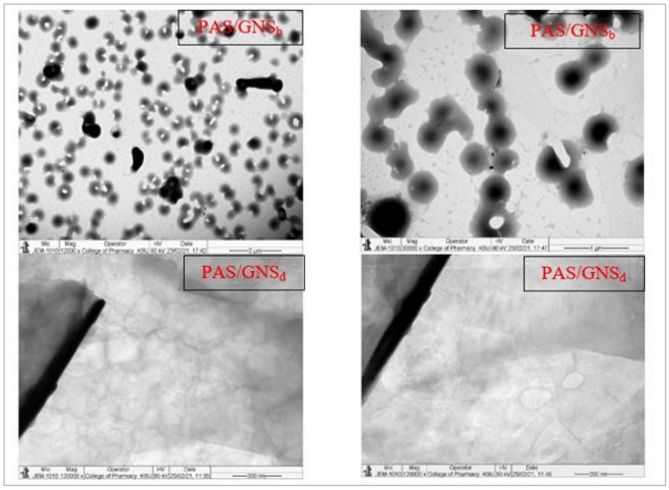

Figure 6. TEM images for PAS/GNS$_b$ and PAS/GNS$_d$.

3. Materials and Methods

3.1. Measurements

Melting points described for two monomers are evaluated on An Automated Melting Point System Device with a Digital Image Processing Technology. The FT.IR measurements were recorded on an IR-470 in the wavenumber range 4000-400 cm^{-1} PerkinElmer. The NMR (^{1}H and ^{13}C) spectra were conducted on Brucker Advanced 850 MHz CRYO PROBE 4 CHANNELS 1H 31P 13C 15N using DMSO-d_6 and $CDCl_3$ as a solvent without TMS. The solubility of PAS was inspected at room temperature using various solvents. A mixture of 0.05 g of the solid polymer with 1 ml of the selected solvent and the solution was analyzed by visual examination. Tetrahydrofuran (THF), dimethyl sulfoxide (DMSO), acetone, benzene (C_6H_6), chloroform ($CHCl_3$), dimethylformamide (DMF), dichloromethane (CH_2Cl_2), concentrated formic acid, and concentrated sulfuric acid were used as selected solvents. Gel permeation chromatography used to determine the molecular weights and molecular weight distributions were performed by Agilent-GPC manufacturing by Agilent Technologies furnished with a differential refractive index detector. The Eluent was DMF at a flow rate of 1.0 ml/min, and the reference polymer was

polystyrene and polymethylmethacrylate. The GPC tools was run with the following conditions: flow rate = 2.000 ml/min, injection volume = 100.000 µL, and sample concentration = 1.000 g/L. The XRD diffractograms of the pure polyamide and its related PAS/GNS$_{a-d}$ nanocomposites were conducted on a (Mannai Technical Services) X-ray Diffractometer model type (RIGAKU ULTIMA_IV) with Ni-filtered CuKα radiation. The last measurements were registered at 40 kV and 40 mA over a scanning range (2θ) between 10°- 80° at a scan speed/duration time of 4.0000 deg/min. The thermogravimetric analysis TGA for pure polymer and its nanocomposites PAS/GNS$_{a-d}$ was examined on a DTG-60H analyzer. All samples were tested in a nitrogen atmosphere and heated up to 800°C at 10°C/min. The morphological topographies of selected samples PAS/GNS$_{b,d}$ composites were estimated via SEM and TEM. Field emission scanning electron microscopy FESEM (Jeol JSM-7600F) using Quanta 250 coating with gold alloy. The TEM measurements were examined only for PAS/GNS nanocomposites (b-d) using a JEM.1010 High-Resolution model at 25X magnification and 100 kV.

3.2. Reagents and solvents

Graphene nano-sheets were obtained from NANO TECH Co. LTD Egypt. Aliphatic diacid chloride (sebacoyl chloride) from (Sigma-Aldrich), 97%. Chloroacetyl chloride and diphenylsulfide from (Merck) were used as purchased. Anhydrous Aluminum chloride $AlCl_3$ from (Sigma-Aldrich) was used as received. Carbon disulfide CS_2 dried over molecular sieves 5Å overnight (Merck). Dimethyl formamide DMF dried over molecular sieves 5Å for two days (Merck). Thiourea, anhydrous potassium carbonate K_2CO_3, sodium hydrogen carbonate $NaHCO_3$, and anhydrous sodium acetate CH_3COONa were obtained from (Fluka). Methanol absolute 99.8% and ethanol absolute 99.9% from (Fisher Chemical) were used as purchased. Concentration hydrochloric acid and acetone were purchased from BDH. All chemicals (solvents or reagents) were high purity (99-98-97%) and were used without any extra purification. Distilled water was used in all experimental studies.

3.3. Monomer synthesis

3.3.1. Bis-4-chloroacetyl-diphenylsulfide (M1)

The titled compound was prepared as described in previous literature [24]. As presented in Figure 7.

3.3.2. 2-Aminothiazole-diphenylsulfide (M2)

The titled compound was prepared as described in previous literature [25]. As presented in Figure 7.

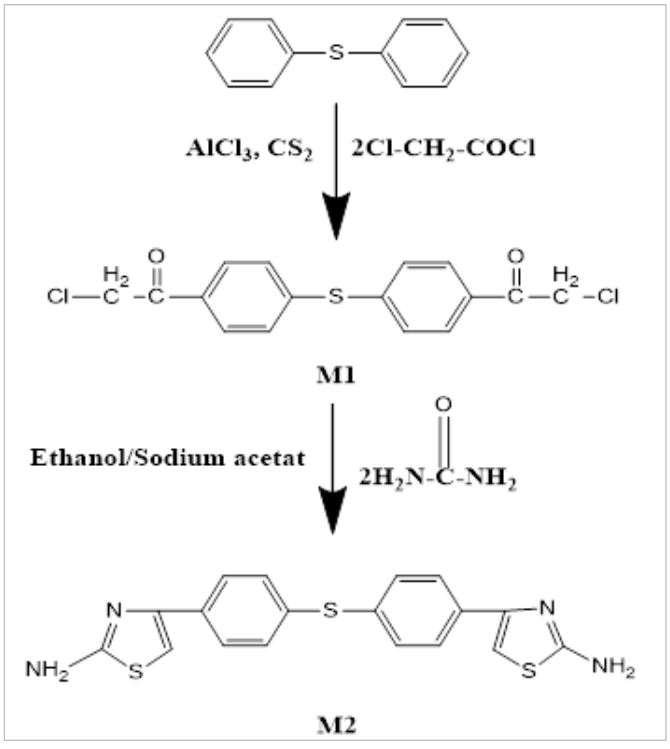

Figure 7. Synthesis of bis-4-chloroacetyl-diphenylsulfide (M1) and 2-aminothiazolediphenylsulfide (M2) monomers.

3.4. Polymer synthesis

3.4.1. Polymerization process (diacid chloride) synthesis of polyamide polymers PAS

Polyamide containing thiazole units and sulfur linkages was synthesized as follows: a mixture of monomer M2 (0.002 moles) was dissolved in 15 ml dry DMF with (0.5 g) anhydrous K_2CO_3 as a catalyst. The previous mixture was added to three-necked round flask connected with a condenser under a nitrogen atmosphere. Besides, a solution of (0.004 moles) sebacoyl chloride was dissolved in 15 ml DMF and added in a small portion under stirring at 0°C. After that, the polymerization was done at room temperature for 10-12 hours, as illustrated in Figure 8. Then, added the produced solution into ice water to give a white-brownish precipitate (PAS). A recently prepared dilute solution of $NaHCO_3$ (5%, 100 ml) was poured. The solid polymer was separated by filtration and all unreacted monomer and biproducts had been removed by washed with distilled water, ethanol, and acetone. The polymer product had been dehydrated at 70°C under reduced pressure (1mmHg) for two days [31]. The FT.IR spectrum for new product displayed the characteristic absorption bands at 3124 cm^{-1} according to the (NH of the secondary amino group) amides. Besides, the other characteristic absorption bands at 1615 cm^{-1} (C=O of carbonyl amide bond) as exhibited in Figure 2.

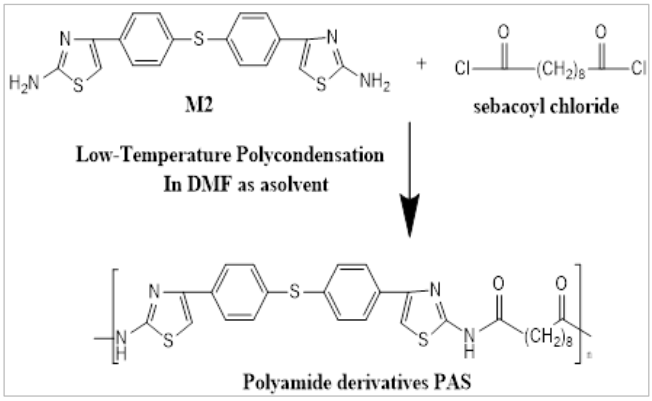

Figure 8. synthesis of polyamide derivative (PAS).

3.4.2. Polyamide-based GNS nanocomposites fabricated process

The PAS/GNS$_{a-d}$ were synthesized using an in-situ polymerization method depending basically on a low-temperature polycondensation process. This process has occurred in a saturated nitrogen atmosphere at every step of the interaction for 10-12 h, and the rest procedure was achieved as same as the way that for the synthesis of pure PAS discussed in the previous section. First, graphene nano-sheets loadings of 1%, 3%, 5%, and 10% were appointed for each composite, as shown in Table 4. The PAS/GNS$_{a-d}$ were synthesized by suspended GNS (1%, 3%, 5%, and 10%) into (M2) 2-aminothiazole diphenylsulfide (0.002 moles) all dissolved in 20 ml dry DMF with (0.5g) K_2CO_3 anhydrous, then the mixture was ultrasonicated for 15 min. Second, the other mixture was prepared by dissolved (0.004 moles) sebacoyl chloride in 15 ml dry DMF were added to the first mixture in a drop-wise manner with stirred during the addition. Third, a recently prepared dilute solution of $NaHCO_3$ (5%, 100 ml) was poured at the end of the reaction. The obtained nanocomposites were separated out by filtration, all unreacted monomer and biproducts were removed by washed with distilled water, ethanol, and acetone. Finally, the desired products were dried under vacuum (1mmHg) at 70°C for 48h as presented in Figure 1.

Table 4. Polyamide and its related GNS doped nanocomposites symbols and codes.

code	G nano-sheets (%)	GNS wt. (g)
PAS	0	0
PAS/GNS$_a$	1	0.002
PAS/GNS$_b$	3	0.006
PAS/GNS$_c$	5	0.01
PAS/GNS$_d$	10	0.02

4. Conclusion

In summary, a novel polyamide containing thioether and thiazole units and its nanocomposites were successfully synthesized by the low-temperature polycondensation method in high yield. Prior to the

polymerization reaction, a new monomer, namely 2-aminothiazole diphenylsulfide, was prepared. The desired polyamide and PAS/GNS$_{a-d}$ nanocomposites structures were confirmed through FT.IR and characterized by XRD, TGA, SEM and TEM. The TGA values indicated a great enhancement in the thermal stability of polyamide and its PAS/GNS$_{a-d}$ nanocomposites, with increasing the proportion of the GNS graphene nano-sheets. Comparing PAS/GNS$_{a-d}$ nanocomposites to pure polymer, thermogravimetric analysis exposed high thermal stability for all PAS/GNS$_{a-d}$ nanocomposites. The SEM images showed a flower-shape in high and low magnifications these morphological behaviors offered excellent distribution of GNS on polyamide surface.

Funding: "This research received no external funding"

Acknowledgments: I would like to thank The King Fahad Medical Research Center for using their laboratory.

Conflicts of Interest: "The authors declare no conflict of interest

References

[1] T. Patel, J. Zhou, J. M. Piepmeier, W. M. Saltzman, Polymeric nanoparticles for drug delivery to the central nervous system, *Advanced drug delivery reviews*, (2012), 64(7), 701-705. https://doi.org/10.1016/j.addr.2011.12.006.

[2] K. E. Lee, N. Morad, T. T. Teng, B. T. Poh, Development, characterization and the application of hybrid materials in coagulation/flocculation of wastewater: A review, *Chemical Engineering Journal*, (2012), 203, 370-386. https://doi.org/10.1016/j.cej.2012.06.109.

[3] B. M. Abu-Zied, M. A. Hussein, A. M. Asiri, Development and characterization of the composites based on mesoporous MCM-41 and polyethylene glycol and their properties, *Composites Part B: Engineering*, (2014), 58, 185-192. https://doi.org/10.1016/j.compositesb.2013.10.071.

[4] M. Gabal, M. Hussein, A. Hermas, Synthesis, characterization and electrical conductivity of polyaniline-Mn0. 8Zn0. 2Fe2O4 nano-composites, *Int. J. Electrochem. Sci*, (2016), 11, 4526-4538. DOI: 10.20964/2016.06.20.

[5] M. M. Rahman, M. A. Hussein, K. A. Alamry, F. M. Al-Shehry, A. M. Asiri, Polyaniline/graphene/carbon nanotubes nanocomposites for sensing environmentally hazardous 4-aminophenol, *Nano-Structures & Nano-Objects*, (2018), 15, 63-74. https://doi.org/10.1016/j.nanoso.2017.08.006

[6] D. F. Katowah, M. A. Hussein, M. M. Rahman, Q. A. Alsulami, M. Alam, A. M. Asiri, Fabrication of hybrid PVA-PVC/SnZnOx/SWCNTs nanocomposites as Sn^{2+} ionic probe for environmental safety, *Polymer-Plastics Technology and Materials*, (2020), 59(6), 642-657. https://doi.org/10.1080/25740881.2019.1673409.

[7] M. A. Hussein, K. A. Alamry, S. J. Almehmadi, M. Elfaky, H. Džudžević-Čančar, A. M. Asiri, M. A. Hussien, Novel biologically active polyurea derivatives and its TiO_2-doped nanocomposites, *Designed monomers and polymers*, (2020), 23(1), 59-74. https://doi.org/10.1080/15685551.2020.1767490.

[8] Y. Chen, X. Li, J. Gao, M. Yang, Y. Liu, Y. Liu, X. Tang, Carbon layer-modified mesoporous silica supporter for PEG to improve the thermal properties of composite phase change material, *Journal of Materials Science*, (2021), 56(9), 5786-5801. https://doi.org/10.1007/s10853-020-05638-8.

[9] S. Lee, O. Kwon, Y. Kang, S. Song, Styrene butadiene rubber/clay nanocomposites for tire tread application, *Plastics, Rubber and Composites*, (2016), 45(9), 382-388. https://doi.org/10.1080/14658011.2016.1209622.

[10] M. Muda, M. Ramli, S. M. Isa, D. Halin, L. Talip, N. Mazelan, N. Anhar, N. Danial, Structural and morphological investigation for water-processed graphene oxide/single-walled carbon nanotubes hybrids, IOP Conference Series: *Materials Science and Engineering*, IOP Publishing, (2017), p. 012030. DOI:10.1088/1757-899X/209/1/012030.

[11] A. Kausar, Corrosion prevention prospects of polymeric nanocomposites: A review, *Journal of Plastic Film & Sheeting*, (2019), 35(2), 181-202. http://dx.doi.org/10.1177/8756087918806027.

[12] V. K. Thakur, R. K. Gupta, Recent progress on ferroelectric polymer-based nanocomposites for high energy density capacitors: synthesis, dielectric properties, and future aspects, *Chemical reviews*, (2016), 116(7), 4260-4317. https://doi.org/10.1021/acs.chemrev.5b00495.

[13] S. Mallakpour, A. Jarahiyan, An eco-friendly approach for the synthesis of biocompatible poly (vinyl alcohol) nanocomposite with aid of modified CuO nanoparticles with citric acid and vitamin C: mechanical, thermal and optical properties, *Journal of the Iranian Chemical Society*, (2016), 13(3), 509-518. DOI:10.1007/s13738-015-0760-3.

[14] M.A. Hussein, W.A. El-Said, B.M. Abu-Zied, J.-W. Choi, Nanosheet composed of gold nanoparticle/graphene/epoxy resin based on ultrasonic fabrication for flexible dopamine biosensor using surface-enhanced Raman spectroscopy, *Nano convergence*, (2020), 7(1), 1-12. https://doi.org/10.1186/s40580-020-00225-8.

[15] Q. Yan, B. Chen, L. Cao, K. Liu, S. Li, L. Jia, K. Kondoh, J. Li, Improved mechanical properties in titanium matrix composites reinforced with quasi-continuously networked graphene nanosheets and in-situ formed carbides, *Journal of Materials Science & Technology*, (2022), 96, 85-93. https://doi.org/10.1016/j.jmst.2021.03.073.

[16] P. Nguyen, Synthesis and characterization of novel polyamides, 2016.

[17] M. T Chhabria, S. Patel, P. Modi, P. S Brahmkshatriya, Thiazole: A review on chemistry, synthesis and therapeutic importance of its derivatives, *Current topics in medicinal chemistry*, (2016), 16(26), 2841-2862. DOI:10.2174/1568026616666160506130731.

[18] S. Nayak, S. L. Gaonkar, A review on recent synthetic strategies and pharmacological importance of 1, 3-thiazole derivatives, *Mini reviews in medicinal chemistry*, (2019), 19(3), 215-238. DOI: 10.2174/1389557518666180816112151.

[19] A. Leoni, A. Locatelli, R. Morigi, M. Rambaldi, Novel thiazole derivatives: a patent review (2008–2012; Part 1), *Expert opinion on therapeutic patents*, (2014), 24(2), 201-216. https://doi.org/10.1517/13543776.2014.858121.

[20] J. Rezania, M. Hayatipour, A. Shockravi, M. Ehsani, V. Vatanpour, Synthesis and characterization of soluble aromatic polyamides containing double sulfide bond and thiazole ring, *Polymer Bulletin*, (2019), 76(3), 1547-1556. https://doi.org/10.1007/s00289-018-2441-8.

[21] S. M. Albukhari, M. A. Hussein, M. A. Abdel Rahman, H. M. Marwani, Highly selective heteroaromatic sulfur containing polyamides for Hg^{+2} environmental remediation, *Designed Monomers and Polymers*, (2020), 23(1), 25-39. https://doi.org/10.1080/15685551.2020.1727172.

[22] M. A. Hussein, R. M. El-Shishtawy, A. Y. Obaid, M. Abdel Salam, Influence of single-walled carbon nanotubes on the performance of poly (azomethine-ether) composite materials, *Polymer-Plastics Technology and Engineering*, (2018), 57(11), 1150-1163. https://doi.org/10.1080/03602559.2017.1373399.

[23] M. A. Hussein, R. M. El-Shishtawy, A. Y. Obaid, The impact of graphene nano-plates on the behavior of novel conducting polyazomethine nanocomposites, *RSC advances*, (2017), 7(17), 9998-10008. https://doi.org/10.1039/C6RA28756E.

[24] M. Abbady, K. Aly, S. Mahgoub, M. Hussein, New polymer syntheses: XV. Synthesis and characterization of new polyketoamine polymers containing ether or thioether linkages in the main chain, *Polymer international*, (2005), 54(11), 1512-1523. https://doi.org/10.1002/pi.1877.

[25] K. Aly, M. Abbady, S. Mahgoub, M. Hussein, Liquid crystalline polymers IX Main chain thermotropic poly (azomethine–ether) s containing thiazole moiety linked with polymethylene spacers, *J Express Polym Lett*, (2007), 1(4), 197-207. DOI: 10.3144/expresspolymlett.2007.31.

[26] M. A. Hussein, Eco-friendly polythiophene (keto-amine) s based on cyclopentanone moiety for environmental remediation, *Journal of Polymers and the Environment*, (2018), 26(3), 1194-1205. DOI 10.1007/s10924-017-1023-4.

[27] M. A. Hussein, M. M. Rahman, A. M. Asiri, Erratum to "Novel Facial Conducting Polyamide-Based Dithiophenylidene Cyclyhexanone Moiety Utilized for Selective Cu^{2+} Sensing", *Polymer-Plastics Technology and Engineering*, (2018), 57(15) 1607-1621. https://doi.org/10.1080/03602559.2017.1409936.

[28] S. J. Almehmadi, K. A. Alamry, M. Elfaky, S. Alqarni, J. Samah, M. A. Hussein, Zinc oxide doped arylidene based polyketones hybrid nanocomposites for enhanced biological activity, *Materials Research Express*, (2020), 7(7), 075302. https://doi.org/10.1088/2053-1591/aba0e8.

[29] Y. Ma, X. Li, W. Zhou, L. Yang, P. Wu, Reinforcement of graphene nanosheets on the microstructure and properties of Sn58Bi lead-free solder, *Materials & design*, (2017), 113, 264-272. https://doi.org/10.1016/j.matdes.2016.10.034.

[30] D. F. Katowah, Q. A. Alsulami, M. Alam, S. H. Ismail, A. M. Asiri, G. G. Mohamed, M. M. Rahman, M. A. Hussein, The Performance of Various SWCNT Loading into CuO–PMMA Nanocomposites Towards the Detection of Mn 2+ Ions, *Journal of Inorganic and Organometallic Polymers and Materials*, (2020), 30, 5024-5041. https://doi.org/10.1007/s10904-020-01591-w.

[31] M. A. Hussein, A. M. Asiri, K. I. Aly, New polyamides and polyoxazoles based on diphenyl ether segments in the polymers' backbone, *International Journal of Polymeric Materials*, (2012), 61(2), 154-175. https://doi.org/10.1080/00914037.2011.593059.